Myocardin-Related Transcription Factors and SRF are required for cytoskeletal dynamics, invasion and experimental metastasis

Souhila Medjkane^, **Cristina Perez-Sanchez^,¶**, **Cedric Gaggioli***, **Erik Sahai***, and **Richard Treisman^,#**

^Transcription Laboratory, Cancer Research UK London Research Institute, Lincoln's Inn Fields Laboratories, 44 Lincoln's Inn Fields, London WC2A 3PX, UK

*Tumour Biology Laboratory, Cancer Research UK London Research Institute, Lincoln's Inn Fields Laboratories, 44 Lincoln's Inn Fields, London WC2A 3PX, UK

Abstract

Rho GTPases control cytoskeletal dynamics through cytoplasmic effectors, and regulate transcriptional activation by the Myocardin Related Transcription Factors (MRTFs), coactivators for Serum Response Factor (SRF). We used RNAi to investigate the contribution of the MRTF-SRF pathway to cytoskeletal dynamics in MDA-MB-231 breast carcinoma and B16F2 melanoma cells, where basal MRTF-SRF activity is Rho-dependent. Depletion of MRTFs or SRF reduces cell adhesion, spreading, invasion and motility in culture, without affecting proliferation or inducing apoptosis; MRTF-depleted tumor cell xenografts exhibit reduced cell motility but proliferate normally. MRTF- and SRF-depleted tumor cells fail to colonise the lung from the bloodstream, being unable to persist following their initial arrival at the lung. Only a few genes exhibit MRTF-dependent expression in both cell lines. Two of these, MYH9 (MLC2) and MYL9 (NMHCIIa), are also required for invasion and lung colonisation. Conversely, expression of an activated MRTF increases lung colonisation by poorly metastatic B16F0 cells. Actin-based cell behaviour and experimental metastasis thus requires Rho-dependent nuclear signalling through the MRTF-SRF network.

Keywords

actin; myosin; metastasis; Rho; SRF; MAL; MRTF

Rho GTPases control the dynamics of the cytoskeleton through multiple effector proteins that regulate the assembly, activity and turnover of actin-based structures, thereby controlling cell adhesion, morphology and motility1–3. Rho signaling, especially through

RhoC and its effector kinase ROCK, is strongly implicated in cancer metastasis[4–8], and this is generally thought to reflect direct effects on the cytoskeleton[2,3]. In addition to such direct cytoplasmic role of Rho effectors in cytoskeletal regulation, Rho GTPases also control activity of MAL/MRTF-A and MKL2/MRTF-B (the MRTFs, myocardin-related transcription factors), transcriptional coactivators of the transcription factor SRF (Serum Response Factor)[9,10]. Rho signaling controls MRTF activity by regulating the availability of G-actin, whose binding to the MRTF N-terminal RPEL domain inhibits MRTF nuclear import, promotes MRTF nuclear export, and inhibits activation by the MRTF-SRF complex[10–12]. In fibroblasts, both basal and growth factor-induced MRTF activity is dependent on functional Rho[9,10].

Many SRF target genes encode cytoskeletal components, including actin itself (for overview see [13]). The control of MRTF activity by Rho thus potentially provides a mechanism by which cytoskeletal gene expression can be coordinated with cytoskeletal regulation. Indeed, SRF null cells exhibit defects in adhesion and migration[14,15], and MRTF signaling is required for fly border cell migration[16] and neuronal guidance in mouse forebrain[17]. However, the notion that transcriptional regulation via the Rho-actin-MRTF-SRF nuclear signalling pathway is required in addition to Rho-controlled cytoplasmic events for effective execution of cytoskeletal remodelling has remained untested.To address this issue directly, elucidate its significance for tumour metastasis, we studied the role of MRTF-SRF signalling in two highly metastatic tumour cell lines, human MDA-MB-231 breast carcinoma and mouse B16F2 melanoma. Rho and its effectors are required for invasion and migration in both cell lines[4,18–22]. MDA-MB-231 cells express high levels of RhoA-GTP, and their metastasis, which requires RhoA and RhoC, is dependent on SDF1/CXCR4-induced actin polymerisation[23–25]. Similarly, the *in vivo* selection of the highly metastatic mouse B16F2 melanoma cell line resulted in increased expression of RhoC[4].

Results

We first assessed the role of Rho-actin signalling to the MRTFs and SRF in the two tumour cell lines. MRTF proteins in MDA-MB-231 cells were predominantly nuclear even under resting conditions, and this was dependent on active Rho, while MRTFs in resting B16F2 cells were cytoplasmic and only accumulated in the nucleus upon stimulation, as previously observed in other cells[10] (Figure 1A; see Discussion). In both cell types, however, the ability of MAL/MRTF-A to activate an SRF reporter gene was substantially dependent on functional Rho, and was also inhibited by co-expression of the nonpolymerisable actin mutant R62D, and by Latrunculin treatment (Figure 1B). Mutationally activated forms of both RhoA and RhoC also activated the SRF reporter gene in both cell types (Figure 1C). MRTF and SRF activity is thus dependent on Rho-actin signalling in these cells.

We developed RNAi approaches to deplete MRTF and SRF in the two cell lines. To activate the MRTF-SRF pathway we used cytochalasin D treatment, which disrupts MRTF association with G-actin[10,12], activating SRF reporter gene expression independently of functional Rho (Figure 1D). CD stimulation activates MRTF/SRF-dependent gene expression, as discussed further below. CD-stimulated reporter activity in MDA-MB-231 cells was partially inhibited by depletion of either MAL/MRTF-A or MKL2/MRTF-B, while

simultaneous knockdown of both MRTFs, or SRF itself, reduced reporter activity to background level (Figure 1E). Reporter activation by activated Rho GTPases was also MRTF-dependent (Figure 1C). Both MRTF proteins thus contribute to SRF reporter activity in these tumour cells, as observed in NIH3T3 fibroblasts7 (S.M., and R.T., in preparation). We established subclones of MDA-MB-231 and B16F2 cells expressing tetracycline-inducible MRTF- and SRF-specific shRNAs (Figure 1F; Figure S1A, S1B). In both cell types, a significant inhibition of SRF reporter activity in the absence of tetracycline became effectively complete upon shRNA induction (Figure 1F; Figure S1A).

Adhesion and spreading require MRTF-SRF activity

Adhesion of MDA-MB-231 cells to fibronectin or collagen matrices was significantly reduced upon simultaneous depletion of both MRTFs, or SRF, in short-term depletion assays (Figure 2A, left). The stable MDA-MB-231 shRNA cell lines exhibited a mild impairment of adhesion 30 minutes following plating which was exacerbated upon tetracycline treatment (Figure 2A, Figure S2). Three hours after plating, MDA-MB-231 control cells had spread efficiently on either matrix (Figure 2B; Figure S2), exhibiting lamellar protusions, stress fiber-like actin bundles, and punctate peripheral paxillin staining (Figure 2C). In contrast, even in the absence of tetracycline, the MDA-MB-231 MRTF shRNA cell lines exhibited decreased spreading, with a reduction in punctate paxillin staining and stress-fibers; upon complete MRTF depletion, MDA-MB-231 cells remained rounded, and punctate paxillin staining and F-actin bundles were effectively absent at 3h (Figure 2B, 2C). These phenotypes were transient, the cells assuming a fully spread morphology by 10h after plating (data not shown). SRF-depleted cells exhibited similar behaviour, consistent with the notion that SRF mediates MRTF activity (Figure 2D). In B16F2 cells, MRTF depletion also impaired cell spreading (Figure 2E).

MRTF-SRF signalling is required for cell motility

We used the scratch-wound assay to assess the requirement for MRTF-SRF signaling in cell motility. Short-term depletion of both MRTFs from MDA-MB-231 cells caused a marked decrease in cell speed (Figure 3A). Similar results were obtained with the stable MDA-MB-231 MRTF shRNA cell lines, and also in B16F2 cells (Figure 3B, 3C, 3E). Consistent with MRTFs acting via SRF, depletion of SRF, both in short-term assays in MDA-MB-231 cells, and in stable SRF shRNA clones, also lowered migration speed (Figure 3A, 3D, 3E). The cell lines exhibited different sensitivity to MRTF depletion: in MDA-MB-231 15-17 cells migration speed was reduced only in the presence of tetracycline, while 15-20 cells and the B16F2 derivatives exhibited substantially reduced motility under uninduced conditions.

Control MDA-MB-231 cells migrated with high persistence (vectorial distance travelled/ total distance traversed), mainly perpendicularly to the wound edge, but this was significantly reduced upon short-term depletion of either the MRTFs or SRF (Figure 3F). In many cell lines scratch-wounding induces repositioning of the microtubule organizing center (MTOC) between the leading edge of the cell and the nucleus in cells bordering the wound, giving the cell an overall polarity which contributes to the directionality of movement (for references see 26). Both MDA-MB-231 MRTF shRNA cell lines showed a significant decrease in the proportion of cells with a reoriented MTOC even in the absence of

tetracycline, and MTOC orientation became effectively random upon complete MRTF depletion (Figure 3G, Figure S3). Taken together these results implicate the MRTFs and SRF in control of cell adhesion and migration.

MRTF-SRF signalling is required for invasion

Depletion of MRTFs or SRF using siRNA oligonucleotides resulted in a significant impairment of MDA-MB-231 cells' ability to migrate through collagen-coated membrane toward serum-containing medium in a modified Boyden chamber assay (Figure 4A). Since stromal fibroblasts can play an important role in tumor invasiveness[27,28], we also tested the requirement for MRTF-SRF activity in an organotypic invasion model, in which tumour cells move through collagen gel along tracks generated by stromal carcinoma-associated fibroblasts (CAFs)[29]. Both MDA-MB-231 and B16F2 exhibited CAF-dependent invasive behaviour, although B16F2 cells required greater numbers of CAFs to manifest invasion; in both cell lines invasive behaviour was MRTF- and SRF-dependent (Figure 4B).

MRTFs are required for tumour cell motility *in vivo*

We next examined the role of MRTF-SRF signalling in tumour growth and motility *in vivo*. Depletion of MRTFs or SRF from MDA-MB-231 or B16F2 cells did not affect proliferation rate or promote apoptosis during culture (Figure 4C; Figure S1C,D). Moreover, MRTF- or SRF-depletion neither increased anoikis upon growth in non-adherent conditions, nor sensitised cells to apoptosis upon growth factor deprivation (Figure S1E, F). Consistent with these observations, subcutaneous implantation of MRTF-depleted MDA-MB-231 or B16F2 derivatives in appropriate host mice efficiently induced tumours that grew at rates comparable to control cell tumours (Figure 4D). The cells in the tumours remained proliferative, with MRTF RNA expression substantially suppressed (Figure 4E; Figure S4A). MRTF proteins were present in both nucleus and cytoplasm in MDA-MB-231 tumour sections, and predominantly cytoplasmic in B16F2 tumours (Figure S4B). Since metastasis is associated with cell motility in primary tumours[30,31], we used intravital imaging of tumour cells *in situ*[32] to investigate the motility of MRTF-depleted and control MDA-MB-231 cells stably expressing GFP or CFP (Figure 4F; Supplementary Videos 1-3). MRTF depletion led to an approximately two-fold reduction in the number of motile cells per unit area of tumour (Figure 4G). MRTF-depleted cells exhibited reduced motility in mixed tumours that also contained control cells, indicating that MRTF activity is required cell-autonomously for cell motility *in vivo* (Figure 4G).

MRTFs and SRF are required for experimental metastasis

To further investigate MRTF-SRF signalling in metastasis we measured the ability of MDA-MB-231 or B16F2 cell derivatives to establish lung tumours following intravenous injection into the mouse tail vein. Large numbers of metastatic nodules were observed in animals injected with control MDA-MB-231 or B16F2 cell lines, while few or no tumours were detectable in animals injected with MRTF-depleted cells (Figure 5A, 5B; Figure S4C). Formation of tumours was very sensitive to MRTF depletion, with only MDA-MB-231 clone 15-17 cells showing residual colonisation activity in the absence of doxycycline (data not shown).

To test whether the lack of tumour growth in these experiments reflects a failure of MRTF-depleted cells to colonise the lung, or the defective proliferation of established tumour cell colonies, we studied the initial fate of fluorescently-labelled control and MRTF-depleted MDA-MB-231 cells, co-injected in equal numbers. Control and MRTF-depleted cells were present in the lung in 1:1 ratio at 2h following injection, but by 24h the ratio of control to MRTF-depleted cells had increased to 40:1 (Figure 5C). A similar result was obtained with MRTF-depled MTLn3 cells, another breast tumour line that exhibits Rho-dependent metastatic spread33 (Figure 5C, Figure S4D). MRTF depletion did not significantly increase the proportion of tumor cells newly arrived at the lung that were apoptotic, as judged by staining for activated caspase 3 (24.7±3.7% control vs 19.3±1.6% MRTF-depleted; n=3). These results strongly suggest that the failure of MRTF-depleted cells to form lung tumours arises because they are rapidly lost from the organ following their initial arrival (see Discussion).

We also assessed the role of SRF in the experimental metastasis assay. Lungs from mice injected with SRF-depleted MDA-MB-231 or B16F2 cells displayed few metastatic nodules, in contrast to abundant nodule formation observed in animals injected with control cells (Figure 5D). It is thus unlikely that lung colonisation involves MRTF acting through transcription factors other than SRF, as suggested by a recent report34, or a cytoplasmic MRTF function resulting from their interaction with G-actin.

MRTF target genes are required for metastasis

The preceding experiments show that MRTF proteins and SRF are required for cytoskeletal dynamics and experimental metastasis in both MDA-MB-231 breast carcinoma and B16F2 melanoma cells. Reasoning that genes whose expression is MRTF-dependent in both cell lines would be candidates for genes mediating such shared MRTF-dependent cell behaviours, we used microarray analysis to compare the transcriptomes of control and MRTF-depleted MDA-MB-231 and B16F2 cells.

MRTF depletion affected expression of 4.9% and 1.4% of genes in MDA-MB-231 and B16F2 cells respectively (significance cutoff 1.5-fold; Supplementary Table 1A, 1B). Since cytochalasin D can directly activate the MRTFs10,12 (Figure 1D), we also treated control or MRTF-depleted cells with CD for 40 min, and identified further candidate MRTF target genes as those whose CD-induced level was reduced upon MRTF depletion. CD treatment increased expression of only 0.35% and 0.3% genes by more than 1.3-fold in MDA-MB-231 and B16F2 cells respectively, and of these 80% and 55% were affected more than 1.5-fold by MRTF depletion (Supplementary Table 1C, 1D). We compared the two datasets to identify MRTF-dependent genes shared between the two cell lines, defined as those where MRTFdepletion affected either basal expression, CD-induced expression, or both, in both lines according to our significance criteria. Of 25 genes identified this way, expression of 16 was reduced following MRTF-depletion, consistent with MRTFs playing a positive role in their expression. Of these, 10 are either functionally validated SRF target genes or contain a phylogenetically conserved SRF binding site within 5kb of their transcription start site, suggesting that they are direct MRTF targets (Figure 6A). We validated the results using RT-PCR (Figure S5A).

As a first step in the evaluation of the potential contribution of SRF targets to invasion and metastasis, we focussed on the cytoskeletal components MYH9 (NMHC-IIA) and MYL9 (MLC2). These proteins, which are components of the actomyosin contractile apparatus[35,36], have been previously implicated in invasive behaviour in tumor cells[5,37–39]. Depletion of MYH9 or MYL9 singly or in combination neither affected cell cycle progression nor induced cell death in the two cell lines (Figure S6). However, it significantly reduced invasiveness in the Boyden chamber and organotypic assays in MDA-MB-231 cells (Figure 6B, 6C), impaired short-term lung colonisation by MDA-MB-231 cells (Figure 6D) and reduced formation of lung tumours by B16F2 cells in the experimental metastasis assay (Figure 6E). The requirement for MRTF activity in these processes thus at least in part reflects MRTF involvement in MYH9 and MYL9 transcription.

MRTF activity is limiting for experimental metastasis in B16F0 cells

To investigate whether elevation of MRTF activity can be sufficient to promote invasion and metastasis we studied B16F0 cells, the less metastatic parent of the B16F2 cell line[4]. To potentiate MRTF activity in the absence of signal, we expressed an activated form of MRTF-A, MAL-xxx, which does not bind actin[11,12]. MAL-xxx strongly potentiated expression of the SRF reporter in B16F0 cells (Figure 7A), and increased expression of the endogenous *Myl9*, *Myh9*, *Cyr61*, and *Tpm1* genes (Figure 7B), but did not suppress anoikis or affect cell cycle progression (Figure S1F; data not shown). Expressing MAL-xxx, which was predominantly nuclear, induced a strikingly spread morphology characterised by multiple intensely-staining paxillin foci, in contrast to untransfected cells, which were rounded with predominantly cytoplasmic paxillin (Figure 7C); it also significantly enhanced the ability of B16F0 cells to establish tumours in the lung colonisation assay (Figure 7D). Thus, at least in certain cell contexts, potentiation of MRTF activity can be sufficient to promote the cytoskeletal activities required for lung colonisation in experimental metastasis.

Discussion

MRTF-SRF signalling is essential for the effective execution of a number of Rho-dependent cytoskeletal processes, including adhesion, spreading and motility, and is also required in experimental invasion and metastasis models. The MRTF-SRF system provides a means by which gene expression can be coordinated with changes in cellular G-actin levels induced by Rho signalling, and we propose that the pathway acts to generate conditions under which Rho-activated cytoskeletal events can occur effectively (Figure 7E). Rho-induced signaling to the nucleus thus plays an essential indirect role that underpins the direct cytoplasmic role played by Rho GTPase effectors in cytoskeletal remodelling. Our data suggest that the adhesion defects of SRF-null ES cells[14] and the impaired migration of SRF-null neurons in the mouse[15] are likely to reflect defects in the MRTF-mediated response to Rho signaling.

While cell motility is dependent on basal levels of Gα12/13-dependent Rho-mDia signaling[25,40], MTOC reorganisation and fibroblast-led tumour cell invasion are Cdc42- and MRCK-dependent[26,29]. Since Rho, Rac and Cdc42 can all activate SRF via the actin-MRTF pathway[10,41], it is likely that the dependence of cytoskeletal behaviour on MRTFs

reflects integration of signals from multiple Rho-family GTPases. It remains possible, however, that Rho-independent pathways are also involved.

Our data indicate that MRTF and SRF activity can facilitate at least two steps in the metastatic process, and suggest that selection for increased Rho-actin-MRTF signaling is one of the pressures driving enhanced RhoC expression in metastatic human cancer and mouse cancer models4–8. MRTF depletion did not affect growth of primary tumours, but reduced cell motility within the tumour. Since previous studies have shown motility correlates with intravasation30,31, this suggests that MRTF is required for efficient exit from primary tumour sites. At later stages, MRTF and SRF activity is also required for efficient colonisation of the lung from the bloodstream: MRTF-depleted cells can survive and arrive at the organ but fail to persist there. This may reflect defective adhesion to endothelial cells, impaired extravasation, or defective adhesion or spreading within the lung, all of which may promote tumour cell elimination by apoptotic or other mechanisms. In culture MRTF- or SRF-depletion did not sensitise cells to anoikis or increase apoptosis upon growth factor deprivation, and consistent with this, MRTF-depleted cells newly arrived at the lung did not exhibit significantly increased apoptosis compared with controls. Increased cell loss may therefore simply reflect their weakened attachment, although more work is needed to fully characterise its kinetics and mechanism. Use of appropriate mouse cancer models, in conjunction with imaging of MRTF subcellular localisation, MRTF-actin interaction, and SRF reporter activity, will give insights into the stages of the metastatic process at which MRTF activity is rate-limiting for different tumours.

The effects of MRTF depletion are strikingly similar in B16F2 melanoma and MDA-MB-231 breast tumour cells, consistent with MRTFs acting through a shared set of gene targets. The MRTFs appear to act redundantly, at least as far as SRF reporter activation is concerned. Moreover, the similarity of the cytoskeletal phenotypes of MRTF- and SRF-depleted cells suggests that they reflect SRF-mediated action of the MRTFs. Indeed, 10 of the 16 genes that are positively regulated by MRTFs in the two cell lines are known or putative SRF targets, suggesting they are also direct MRTF targets. We therefore think it unlikely our results reflect MRTF signaling through Smads to EMT34; indeed, MRTF depletion did not affect expression of markers or regulators of mesenchymal invasive gene expression in MDA-MB-231 or B16F2 cells (see Figure S5B).

Genomic studies indicate that SRF is a global regulator of cytoskeletal gene expression13, and many of its cytoskeletal targets are controlled through Rho-actin signaling, via the MRTFs41–44. Some encode cytoskeletal components involved in actomyosin-based contractility, including nonmuscle myosin heavy chain (MYH9/NMHC-IIA) and its regulatory light chain (MYL9/MLC2), which have both previously been implicated in tumour cell invasive behaviour, and which are targets of the Rho effector ROCK5, 37–39. Our data indicate that the MRTF/SRF-dependence of cytoskeletal events and experimental metastasis reflects at least in part a requirement for sufficient basal expression of these genes (Figure 7E). The other positively-regulated MRTF targets shared between MDA-MB-231 and B16F2 cells, which are surprisingly few in number, may also play important roles: for example, the CCN proteins Cyr61 and CTGF appear to play pro- and anti-invasive roles in breast cancer45, while Fos has been implicated in skin tumor progression46. A number of

MRTF targets are not affected at basal level but are susceptible to acute activation of the MRTF-SRF pathway. Such activation is likely to occur through Rho signalling during particularly dynamic periods of cytoskeletal remodelling, such as exit from the primary tumour and extravasation at secondary sites: in addition to extracellular stimuli Rho signalling is known to be activated by mechanical stress1, which can induce MRTF nuclear accumulation41–44 (Figure 7E). Intriguingly, MRTF depletion increases expression of 9 genes in both lines: the mechanism underlying this, and the functional role of these genes, awaits elucidation.

At least in certain cell contexts, activity of the MRTF-SRF pathway can be limiting, since expression of constitutively active MRTF-A can promote cell spreading and potentiation of lung colonisation by the poorly metastatic B16F0 cells; further analysis of MRTF expression and activity during tumour progression is therefore warranted. MRTF proteins are substantially nuclear in both MDA-MB-231 and MTLn3 breast tumors, and MRTF proteins are also nuclear in a subset of spontaneous breast tumors (unpublished observations); however, MRTFs are predominantly cytoplasmic in B16F2 cells, so nuclear MRTF localisation is not indicative of metastatic capability *per se*. Indeed, although nuclear localisation of MRTFs is required for their function as transcriptional activators, it is not necessarily sufficient for maximal activity, which requires their dissociation from actin12. It will be interesting to assess systematically how MRTF expression, subcellular localisation, and activity correlates with tumour invasiveness and progression.

Methods

Cell culture, shRNA cell lines, and siRNA treatment

Human MDA-MB-231 breast cancer cells, and mouse B16F0 and B16F2 mouse melanoma cells were maintained in Dulbecco's modified Eagle's medium (DMEM) with 10% fetal calf serum (FCS), and MTLn3 rat breast cancer cells in αMEM containing 5% FCS. For *in vivo* tracking, pooled MDA-MB-231 cell clones stably expressing GFP or CFP from expression plasmids (Clontech) were recovered by FACS and expanded in 100μg/ml neomycin. GFP- and Cherry-expressing MTLn3 cells have been described47. Growth curves were obtained by daily counting for cells growing in 10% serum and compared by 2-way ANOVA. Cell cycle analysis was by standard methods (see Supplementary Information). MDA-MB-231 and B16-F2 derivatives expressing Tet repressor were constructed using pcDNA6/TR (Invitrogen), selecting for Blasticidin resistance (5μg/ml). Clones that exhibited effective Tet-operator-luciferase reporter activation were used to generate shRNA cell lines using pTER-shRNA plasmids48 (see Supplementary Information) selecting for zeocin resistance (200μg/ml). Appropriate MDA-MB-231 and B16F2 shRNA clones were selected for further use following immunoblotting and SRF reporter analysis.

Transfections, reporter assays, siRNA treatments and immunofluorescence

For reporter assays cells in 24-well dishes were transfected with SRF (p3DA-luc) and control (ptk-RL) reporters and analysed as described10 11, 12 For short-term depletions MDA-MB-231 or B16F2 cells were transfected with 190 pmol siRNA oligonucleotides

using Lipofectamine 2000 (Invitrogen; MDA-MB-231) and Plus Reagent (Invitrogen; B16F2).

Whole cell extracts preparation, immunoblotting and immunofluorescence were performed using standard techniques. F-actin was detected with FITC-phalloidin (Invitrogen), and nuclei were visualised using DAPI or PI. For antibodies, see Supplementary Information.

Adhesion-spreading assay

Cells detached using PBS-EDTA (1mM) were plated in dishes coated with Fibronectin (Sigma; 10μg/ml) and Collagen I (BD Biosciences; 50μg/ml) and later processed for fluorescence microscopy or quantitative adhesion assay using BCECF (Invitrogen; manufacturer's protocol).

Scratch-wound assay

Confluent cells previously induced or not with tetracycline were scratch-wounded with a 20μl pipette tip. Cell migration was monitored using time-lapse video microscopy every 5 min or 30min for 48h after scratching using a low-light inverted Zeiss microscope. Cells at the leading edge of the scratch were tracked using Tracker software. Mean speeds were calculated over the recording time for each cell; persistence was measured during successive 50-minute windows for each cell. Migration speed and persistence were evaluated using an algorithm implemented in "Mathematica" software (Wolfram Research, Inc), with hierarchical ANOVA analysis taking into account the nested data structure.

Transwell and organotypic invasion assays

Polycarbonate transwells (8μm pore size) were coated with 3mm deep 2mg/ml collagen gel in serum-free medium/20mM Hepes, and set for 1h. Tetracycline-treated cells were allowed to attach for 2-3h to the underside of the chamber, then whole medium was added to the upper compartment. Cells were allowed to migrate into the collagen matrix for 16h, fixed, stained with PI, and Z-sections taken by confocal microscopy. Invasion index was defined as % migrated cells/initially attached cells.

Organotypic invasion assays through matrix containing CAFs (0.5×10^6/ml for MDA-MB-231; 1.2×10^6/ml for B16F2) were as described[29] (see Supplementary Information). Invasion index was calculated as (1-(non-invading area/total area)).

Tumour growth, metastatic lung assay

Animal experimentation was carried out under UK Home Office Project licence PPL70/5670. Animals were maintained in SPF conditions in the CRUK Biological Resources Unit.

For xenografts, 2×10^6 MDA-MB-231 or 0.2×10^6 B16F2 cells were injected subcutaneously into the fat pad of female nude mice or the flank of C57BL/6 mice respectively, and animals maintained on doxycycline (2mg/ml in water). RNA was extracted using the RNeasy mini-column (QIAGEN). Frozen tumour sections were used for anti-Ki-67 histochemistry (VP-K451,Vector laboratories).

For experimental metastasis assays cells were injected into the tail vein of the appropriate host (1-2x10^6 MDA-MB-231 or 0.3x10^6 B16F2 stable shRNA derivatives; 0.75x10^6 or 0.9x10^6 transiently siRNA-transfected B16F2 or B16F0 cells respectively). Lungs were dissected 12-20 weeks (MDA-MB-231) or 9-14 days (B16F2, B16F0) later, rinsed in PBS and fixed in 10% Neutral-Buffered Formalin solution. MDA-MB-231 lungs were paraffin-embedded, sectioned (4μm thickness, 5 levels, 100μm intervals) H-and-E stained, and metastatic nodules counted. B16F2 lungs were whitened using Fekete's solution (70% ethanol, 8% formaldehyde, 4% acetic acid) and surface metastatic lung nodules counted macroscopically. Results with transiently transfected cells and stable cell lines were comparable, since MRTF-depletion affects an early step in lung colonisation.

Short-term lung colonisation assays used fluorescently-labelled MDA-MB-231 and Mtln3 cell derivatives, transfected with siRNA 24hr prior to use. MRTF-depleted and control cells (0.75 x10^6 each), were injected into the tail vein of nude mice, which were sacrificed 2h or 24h later. Fluorescently-labelled cells at the lung were counted microscopically. MYL9- and MYH9-depleted cells were injected separately; the number of fluorescent cells was normalised to the total lung surface examined. Apoptotic tumor cells were detected by staining paraffin-embedded lung sections with anti-GFP (Abcam AB6673) and anti-caspase 3 (R&D EF835).

Intravital imaging

Female SCID mice (5-6 weeks old) were injected in the mammary fat pad with 10^6 tumor cells and maintained on 2mg/ml doxycycline. When tumours reached 5-7 mm diameter (at 21-26 days) mice were anaesthetised and the tumour exposed[32]. Chameleon Coherent Ti-Sapphire laser was tuned to 870nm for EGFP excitation and to 850nm for ECFP excitation or simultaneous ECFP and EGFP excitation. CFP and GFP and collagen were distinguished as described, and tissue architecture and host cells assessed using a reflectance image collected using a 633nm laser[32]. Typically four different areas, 2-3 sections per area, were imaged for 20-30 minutes in each tumour (4-6 tumours per animal). The number of motile cells that remained visible in the same confocal section for several minutes was counted and normalised to the total area of tumor cells in the section as determined by ECFP or EGFP fluorescence. Cells that moved between sections were not analysed.

Microarray procedures and analysis

Total RNA was prepared using Trizol (Invitrogen) followed by RNeasy purification and cRNA probe generation (Affymetrix GeneChip protocol). MDA-MB-231 clones grown with tetracycline for 7 days were induced by 5μM CD for 40min in two independent cell induction experiments. B16F2 cells were transfected with control or mrtfa/b siRNA oligonucleotides, with a 40min 5μM CD treatment 48h later, in 3 independent experiments. Microarray analysis used U133Plus 2.0 GeneChips (54675 probe-sets, targeting 24317 unique refseq mRNA records, 21008 unique Unigene IDs) and mouse MOE430 2.0 GeneChips (45101 probe-sets, targeting 42945 unique refseq mRNA records, 22640 unique Unigene IDs). Comparative analyses were carried out using the empirical Bayes t-test provided within the 'limma' package to detect differential expression[49]: gene lists were subjected to a false discovery threshold of 0.001 prior to being filtered by fold change.

Genes whose expression was altered >1.5-fold upon depletion were defined as MRTF-dependent. CD-inducible genes were defined as those whose expression changed by >1.3-fold upon stimulation; genes whose CD-induced level was reduced >1.5-fold upon MRTF-depletion were defined as MRTF-dependent. Where multiple probes were interrogated for a gene, the effects of MRTF depletion were taken as the average of the effects for each probe, and for induction by CD, fold induction was taken as the average of the fold inductions for each probe. Only probes covering the same transcripts were included in the analysis. Q-PCR validation was performed using SYBR Green-based real time PCR (invitrogen) as previously described12 (Primer details, Supplementary Information).

Supplementary Material

Refer to Web version on PubMed Central for supplementary material.

Acknowledgments

References

1. Geiger B, Bershadsky A. Assembly and mechanosensory function of focal contacts. Curr Opin Cell Biol. 2001; 13:584–92. [PubMed: 11544027]

2. Sahai E, Marshall CJ. RHO-GTPases and cancer. Nat Rev Cancer. 2002; 2:133–42. [PubMed: 12635176]

3. Yamaguchi H, Condeelis J. Regulation of the actin cytoskeleton in cancer cell migration and invasion. Biochim Biophys Acta. 2007; 1773:642–52. [PubMed: 16926057]

4. Clark EA, Golub TR, Lander ES, Hynes RO. Genomic analysis of metastasis reveals an essential role for RhoC. Nature. 2000; 406:532–5. [PubMed: 10952316]

5. Croft DR, et al. Conditional ROCK activation in vivo induces tumor cell dissemination and angiogenesis. Cancer Res. 2004; 64:8994–9001. [PubMed: 15604264]

6. Hakem A, et al. RhoC is dispensable for embryogenesis and tumor initiation but essential for metastasis. Genes Dev. 2005; 19:1974–9. [PubMed: 16107613]

7. Suwa H, et al. Overexpression of the rhoC gene correlates with progression of ductal adenocarcinoma of the pancreas. Br J Cancer. 1998; 77:147–52. [PubMed: 9459160]

8. van Golen KL, et al. A novel putative low-affinity insulin-like growth factor-binding protein, LIBC (lost in inflammatory breast cancer), and RhoC GTPase correlate with the inflammatory breast cancer phenotype. Clin Cancer Res. 1999; 5:2511–9. [PubMed: 10499627]

9. Cen B, et al. Megakaryoblastic leukemia 1, a potent transcriptional coactivator for serum response factor (SRF), is required for serum induction of SRF target genes. Mol Cell Biol. 2003; 23:6597–608. [PubMed: 12944485]

10. Miralles F, Posern G, Zaromytidou A-I, Treisman R. Actin dynamics control SRF activity by regulation of its coactivator MAL. Cell. 2003; 113:329–42. [PubMed: 12732141]

11. Guettler S, Vartiainen MK, Miralles F, Larijani B, Treisman R. RPEL motifs link the SRF cofactor MAL but not myocardin to Rho signalling via actin binding. Mol Cell Biol. 2007

12. Vartiainen MK, Guettler S, Larijani B, Treisman R. Nuclear actin regulates dynamic subcellular localization and activity of the SRF cofactor MAL. Science. 2007; 316:1749–52. [PubMed: 17588931]

13. Sun Q, et al. Defining the mammalian CArGome. Genome Res. 2006; 16:197–207. [PubMed: 16365378]

14. Alberti S, et al. Neuronal migration in the murine rostral migratory stream requires serum response factor. Proc Natl Acad Sci U S A. 2005; 102:6148–53. [PubMed: 15837932]

15. Schratt G, et al. Serum response factor is crucial for actin cytoskeletal organization and focal adhesion assembly in embryonic stem cells. J Cell Biol. 2002; 156:737–50. [PubMed: 11839767]

16. Somogyi K, Rorth P. Evidence for tension-based regulation of Drosophila MAL and SRF during invasive cell migration. Dev Cell. 2004; 7:85–93. [PubMed: 15239956]

17. Knoll B, et al. Serum response factor controls neuronal circuit assembly in the hippocampus. Nat Neurosci. 2006; 9:195–204. [PubMed: 16415869]

18. Kusama T, Mukai M, Tatsuta M, Nakamura H, Inoue M. Inhibition of transendothelial migration and invasion of human breast cancer cells by preventing geranylgeranylation of Rho. Int J Oncol. 2006; 29:217–23. [PubMed: 16773203]

19. Pille JY, et al. Anti-RhoA and anti-RhoC siRNAs inhibit the proliferation and invasiveness of MDA-MB-231 breast cancer cells in vitro and in vivo. Mol Ther. 2005; 11:267–74. [PubMed: 15668138]

20. Yoshioka K, Foletta V, Bernard O, Itoh K. A role for LIM kinase in cancer invasion. Proc Natl Acad Sci U S A. 2003; 100:7247–52. [PubMed: 12777619]

21. Dua P, Gude RP. Pentoxifylline impedes migration in B16F10 melanoma by modulating Rho GTPase activity and actin organisation. Eur J Cancer. 2008; 44:1587–95. [PubMed: 18495474]

22. Nakajima M, et al. Effect of Wf-536, a novel ROCK inhibitor, against metastasis of B16 melanoma. Cancer Chemother Pharmacol. 2003; 52:319–24. [PubMed: 12783205]

23. Caceres M, Guerrero J, Martinez J. Overexpression of RhoA-GTP induces activation of the Epidermal Growth Factor Receptor, dephosphorylation of focal adhesion kinase and increased motility in breast cancer cells. Exp Cell Res. 2005; 309:229–38. [PubMed: 15963982]

24. Muller A, et al. Involvement of chemokine receptors in breast cancer metastasis. Nature. 2001; 410:50–6. [PubMed: 11242036]

25. Tan W, Martin D, Gutkind JS. The Galpha13-Rho signaling axis is required for SDF-1-induced migration through CXCR4. J Biol Chem. 2006; 281:39542–9. [PubMed: 17056591]

26. Gomes ER, Jani S, Gundersen GG. Nuclear movement regulated by Cdc42, MRCK, myosin, and actin flow establishes MTOC polarization in migrating cells. Cell. 2005; 121:451–63. [PubMed: 15882626]

27. Bhowmick NA, Neilson EG, Moses HL. Stromal fibroblasts in cancer initiation and progression. Nature. 2004; 432:332–7. [PubMed: 15549095]

28. Orimo A, Weinberg RA. Stromal fibroblasts in cancer: a novel tumor-promoting cell type. Cell Cycle. 2006; 5:1597–601. [PubMed: 16880743]

29. Gaggioli C, et al. Fibroblast-led collective invasion of carcinoma cells with differing roles for RhoGTPases in leading and following cells. Nat Cell Biol. 2007; 9:1392–400. [PubMed: 18037882]

30. Wang W, et al. The activity status of cofilin is directly related to invasion, intravasation, and metastasis of mammary tumors. J Cell Biol. 2006; 173:395–404. [PubMed: 16651380]

31. Xue C, et al. Epidermal growth factor receptor overexpression results in increased tumor cell motility in vivo coordinately with enhanced intravasation and metastasis. Cancer Res. 2006; 66:192–7. [PubMed: 16397232]

32. Sahai E, et al. Simultaneous imaging of GFP, CFP and collagen in tumors in vivo using multiphoton microscopy. BMC Biotechnol. 2005; 5:14. [PubMed: 15910685]

33. Bouzahzah B, et al. Rho family GTPases regulate mammary epithelium cell growth and metastasis through distinguishable pathways. Mol Med. 2001; 7:816–30. [PubMed: 11844870]

34. Morita T, Mayanagi T, Sobue K. Dual roles of myocardin-related transcription factors in epithelial mesenchymal transition via slug induction and actin remodeling. J Cell Biol. 2007; 179:1027–42. [PubMed: 18056415]

35. Clark K, Langeslag M, Figdor CG, van Leeuwen FN. Myosin II and mechanotransduction: a balancing act. Trends Cell Biol. 2007; 17:178–86. [PubMed: 17320396]

36. Somlyo AP, Somlyo AV. Ca2+ sensitivity of smooth muscle and nonmuscle myosin II: modulated by G proteins, kinases, and myosin phosphatase. Physiol Rev. 2003; 83:1325–58. [PubMed: 14506307]

37. Betapudi V, Licate LS, Egelhoff TT. Distinct roles of nonmuscle myosin II isoforms in the regulation of MDA-MB-231 breast cancer cell spreading and migration. Cancer Res. 2006; 66:4725–33. [PubMed: 16651425]

38. Dulyaninova NG, House RP, Betapudi V, Bresnick AR. Myosin-IIA heavy-chain phosphorylation regulates the motility of MDA-MB-231 carcinoma cells. Mol Biol Cell. 2007; 18:3144–55. [PubMed: 17567956]

39. Wyckoff JB, Pinner SE, Gschmeissner S, Condeelis JS, Sahai E. ROCK- and myosin-dependent matrix deformation enables protease-independent tumor-cell invasion in vivo. Curr Biol. 2006; 16:1515–23. [PubMed: 16890527]

40. Goulimari P, et al. Galpha12/13 is essential for directed cell migration and localized Rho-Dia1 function. J Biol Chem. 2005; 280:42242–51. [PubMed: 16251183]

41. Sotiropoulos A, Gineitis D, Copeland J, Treisman R. Signal-regulated activation of serum response factor is mediated by changes in actin dynamics. Cell. 1999; 98:159–69. [PubMed: 10428028]

42. Philippar U, et al. The SRF target gene Fhl2 antagonizes RhoA/MAL-dependent activation of SRF. Mol Cell. 2004; 16:867–80. [PubMed: 15610731]

43. Selvaraj A, Prywes R. Expression profiling of serum inducible genes identifies a subset of SRF target genes that are MKL dependent. BMC Mol Biol. 2004; 5:13. [PubMed: 15329155]

44. Morita T, Mayanagi T, Sobue K. Reorganization of the actin cytoskeleton via transcriptional regulation of cytoskeletal/focal adhesion genes by myocardin-related transcription factors (MRTFs/MAL/MKLs). Exp Cell Res. 2007; 313:3432–45. [PubMed: 17714703]

45. Jiang WG, et al. Differential expression of the CCN family members Cyr61, CTGF and Nov in human breast cancer. Endocr Relat Cancer. 2004; 11:781–91. [PubMed: 15613452]

46. Saez E, et al. c-fos is required for malignant progression of skin tumors. Cell. 1995; 82:721–32. [PubMed: 7545543]

47. Pinner S, Sahai E. PDK1 regulates cancer cell motility by antagonising inhibition of ROCK1 by RhoE. Nat Cell Biol. 2008; 10:127–37. [PubMed: 18204440]

48. van de Wetering M, et al. Specific inhibition of gene expression using a stably integrated, inducible small-interfering-RNA vector. EMBO Rep. 2003; 4:609–15. [PubMed: 12776180]

49. Smyth GK. Bioinformatics and Computational Biology Solutions using R and Bioconductor. Gentleman R, Carey V, Dudoit S, Irizarry R, Huber W, editorsSpringer; New York: 2005. 397–420.

50. Li S, Chang S, Qi X, Richardson JA, Olson EN. Requirement of a myocardin-related transcription factor for development of mammary myoepithelial cells. Mol Cell Biol. 2006; 26:5797–808. [PubMed: 16847332]
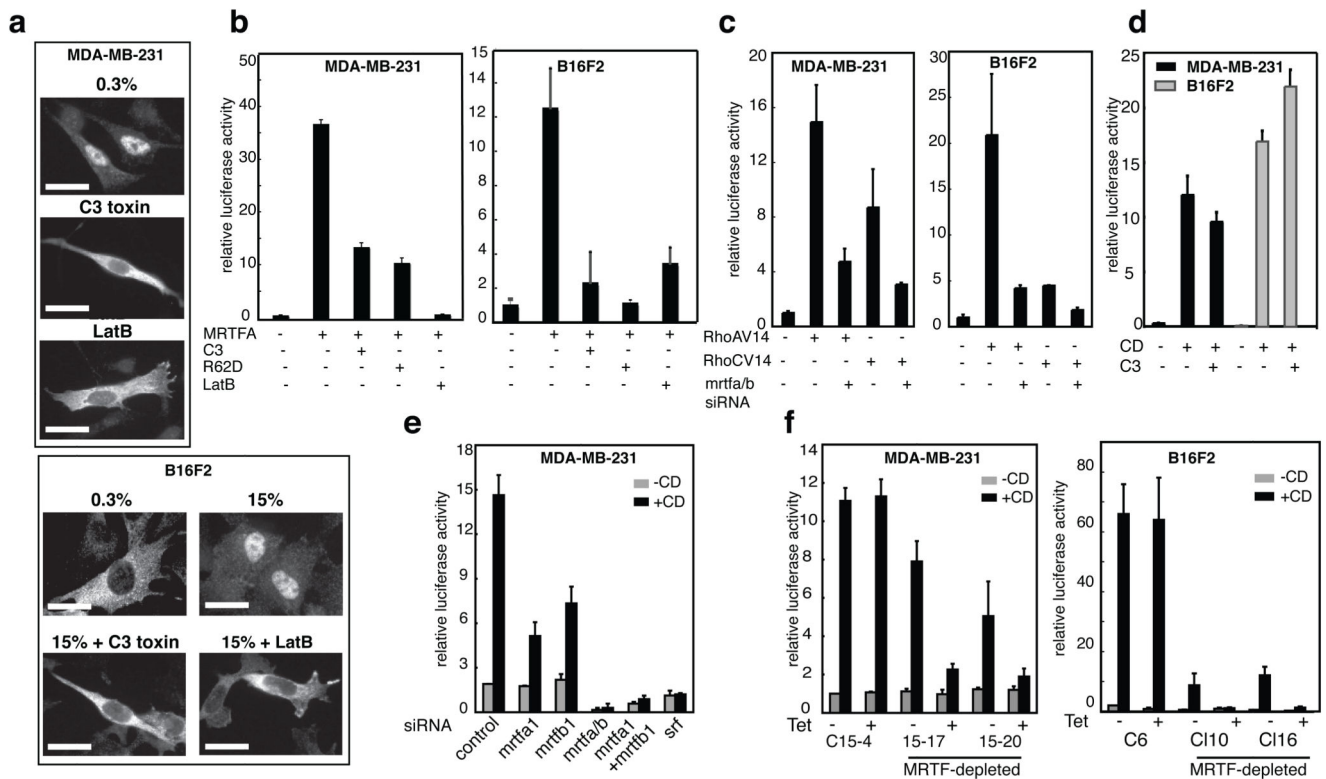
Figure 1. MRTFs and SRF activity is dependent on Rho-actin signalling in MDA-MB-231 and B16F2 cells.

(**A**) MRTF localisation is Rho- and actin-dependent. Cells expressing Flag-MRTF-A with or without C3 transferase where indicated, were stimulated by serum and/or treated with Latrunculin B. Scale bar, 20μm. (**B-E**) SRF reporter gene activity is MRTF- and Rho-actin signal-dependent. Cells were transfected with an SRF reporter gene together with MRTF-A, C3 transferase, and activated RhoA or RhoC expression plasmids as indicated. MRTF and SRF were depleted from MDA-MB-231 cells or B16F2 cells by short term siRNA oligonucleotide transfection (siRNA oligonucleotides: mrtfa1 targets MAL/MRTF-A; mrtfb1 targets MRTF-B; mrtfa1+mrtfb1 and mrtfa/b, simultaneously target both MRTFs, in two different ways; srf targets SRF). Data are mean ± half-range of two independent experiments. (**B**) Basal MRTF activity requires Rho-actin signalling; (**C**) MRTF activation by constitutively active RhoA and RhoC; (**D**) CD stimulation activates the SRF reporter gene even when Rho is inactivated by C3 transferase expression. (**E**) CD-stimulated reporter activity is mediated by MRTF-A, MRTF-B, and SRF. (**F**) Reporter activity in stable cell derivatives expressing tetracycline-inducible MRTF shRNAs. C15-4 cells, MDA-MB-231 parental Tet repressor cell line; 15-17 and 15-20, MDA-MB-231 cell lines expressing the mrtfa/b shRNA; C6 cells, B16F2 parental Tet repressor cell line; Cl10 and Cl16, B16F2 cells expressing the mrtfa/b shRNA. Tetracycline treatment (72h) was as indicated. For cell lines stably expressing inducible SRF shRNAs, see Figure S1A and S1B.
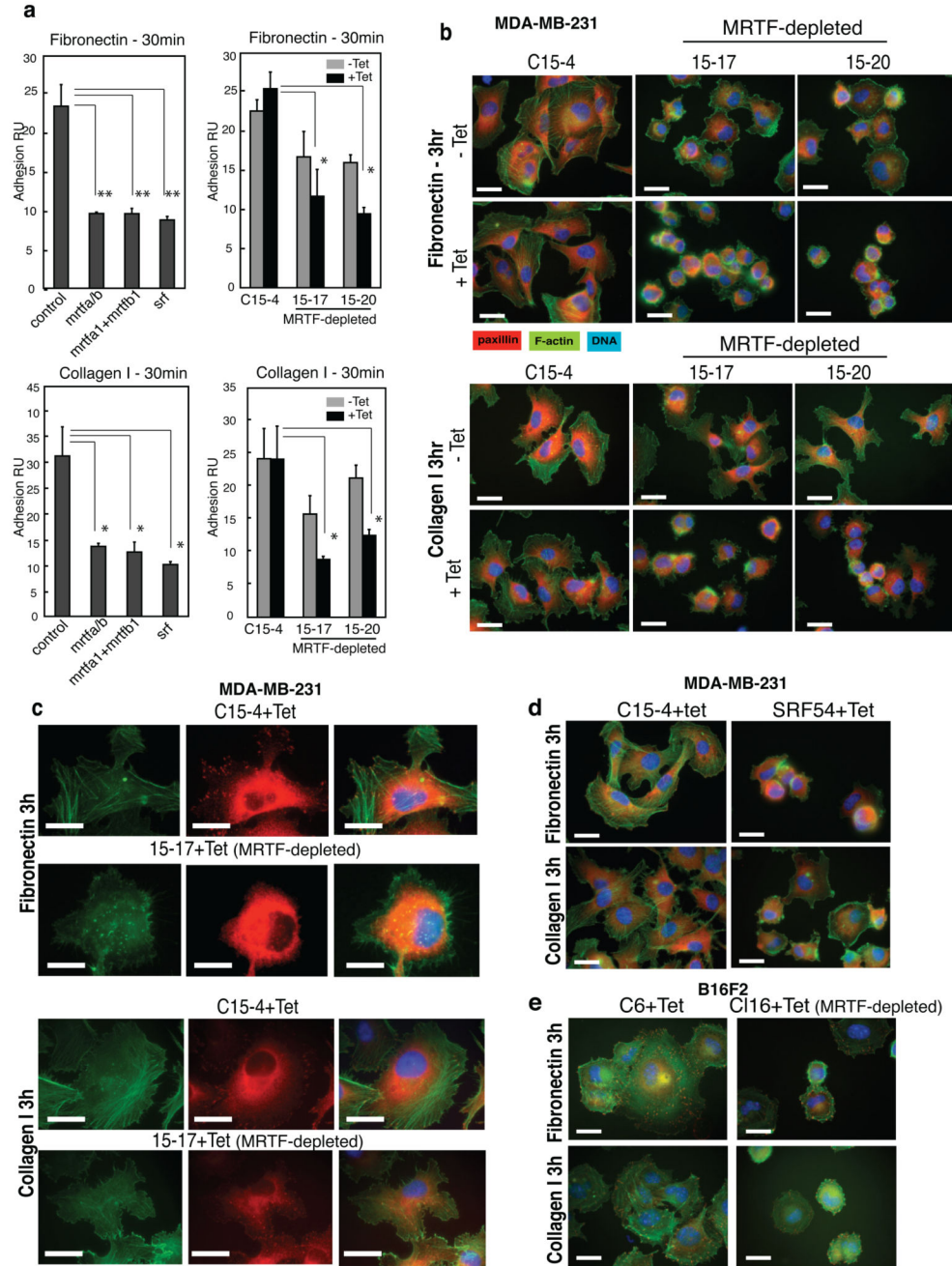
Figure 2. MRTF activity is required for cell adhesion and spreading

(**A**) Adhesion assay. MDA-MB-231 cells depleted of MRTFs or SRF by siRNA oligonucleotide transfection (left panels) or expression of stable MRTF shRNAs (right panels) were plated on fibronectin (top panels) or collagen I (bottom panels), and adhesion quantified by dye retention 30 minutes after plating. Data show mean ± SEM (n=3; **p<0.001, *p<0.05, Student's t test). (**B-D**) Impaired cell spreading in SRF or MRTF depleted MDA-MB-231 cell lines. MDA-MB-231 parental control (C15-4), derivatives expressing MRTF shRNA (15-17, 15-20) or SRF shRNA (SRF54) were plated on

fibronectin or collagen I matrices for 3h, then fixed and stained with anti-paxillin antibody (red) and phalloidin (green) to visualize focal contacts and F-actin respectively. Scale bars, 20μm. **(B),** MRTF depletion; **(C)** high-magnification of representative cells from experiment in **(B)**; **(D),** SRF depletion. **(E)** Impaired B16F2 cell spreading. Parental control C6 or MRTF shRNA C16 cells were analysed as in panel **(B).** For time course, see Figure S2.
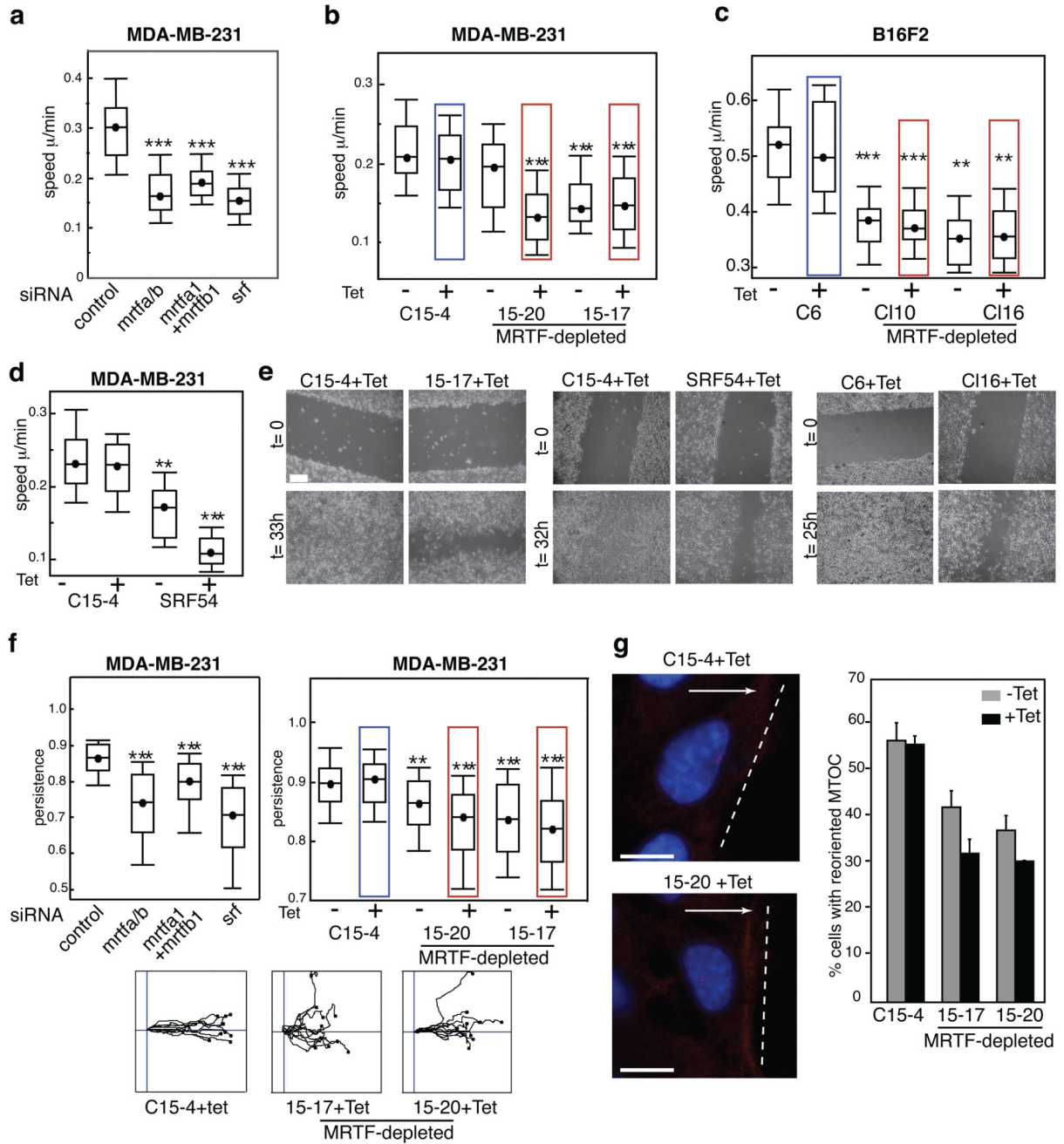
Figure 3. MRTFs and SRF are required for cell motility in culture

(**A-E**) Migration-speed in the scratch-wound assay is MRTF- and SRF-dependent. MRTF
and SRF were depleted from MDA-MB-231 cells (**A, B, D**) or B16F2 cells (**C**) either by
short term siRNA oligonucleotide transfection or in stable cell derivatives expressing
tetracycline-inducible shRNAs, as described in Figure 1 legend. A scratch was made across
the confluent cell monolayer and migration of individual cells monitored using time lapse
microscopy. Median speed was calculated by tracking individual cell movement (~50-150
cells per condition, 3 independent experiments; for hierarchical ANOVA, comparisons were

made between control and depleted cells cultured under comparable conditions, ie either with or without tetracycline. ***, $p<0.001$; **, $p<0.01$; *, $p<0.05$). **(E)** Wound-closure images before and after wounding. MRTF- and SRF-depleted MDA-MB-231, and MRTF-depleted B16F2 cells are shown in left, centre and right images. Scale bars, 200μm. **(F)** Directionality of migration in the scratch-wound assay is MRTF- and SRF-dependent. Median persistence in migrating MDA-MB-231 cells was calculated by tracking individual cells, 3 independent experiments; significance by ANOVA, ***, $p<0.001$; ** $p<0.01$. Bottom, overlays of representative trajectories described by parental control (C15-4) and MRTF-depleted cells. **(G)** MTOC reorientation 6h following scratch-wounding. Cells were fixed and stained for gamma-tubulin to reveal the MTOC as a red dot; nuclei were counterstained with DAPI (blue). Dashed white line, wound edge; arrow, direction of movement. MTOC in the first row of cells migrating into the wound scored as reoriented when located between the nucleus and the leading edge of the cells into the wound. Data are mean ± half-range of two independent experiments. Scale bar, 10μm.
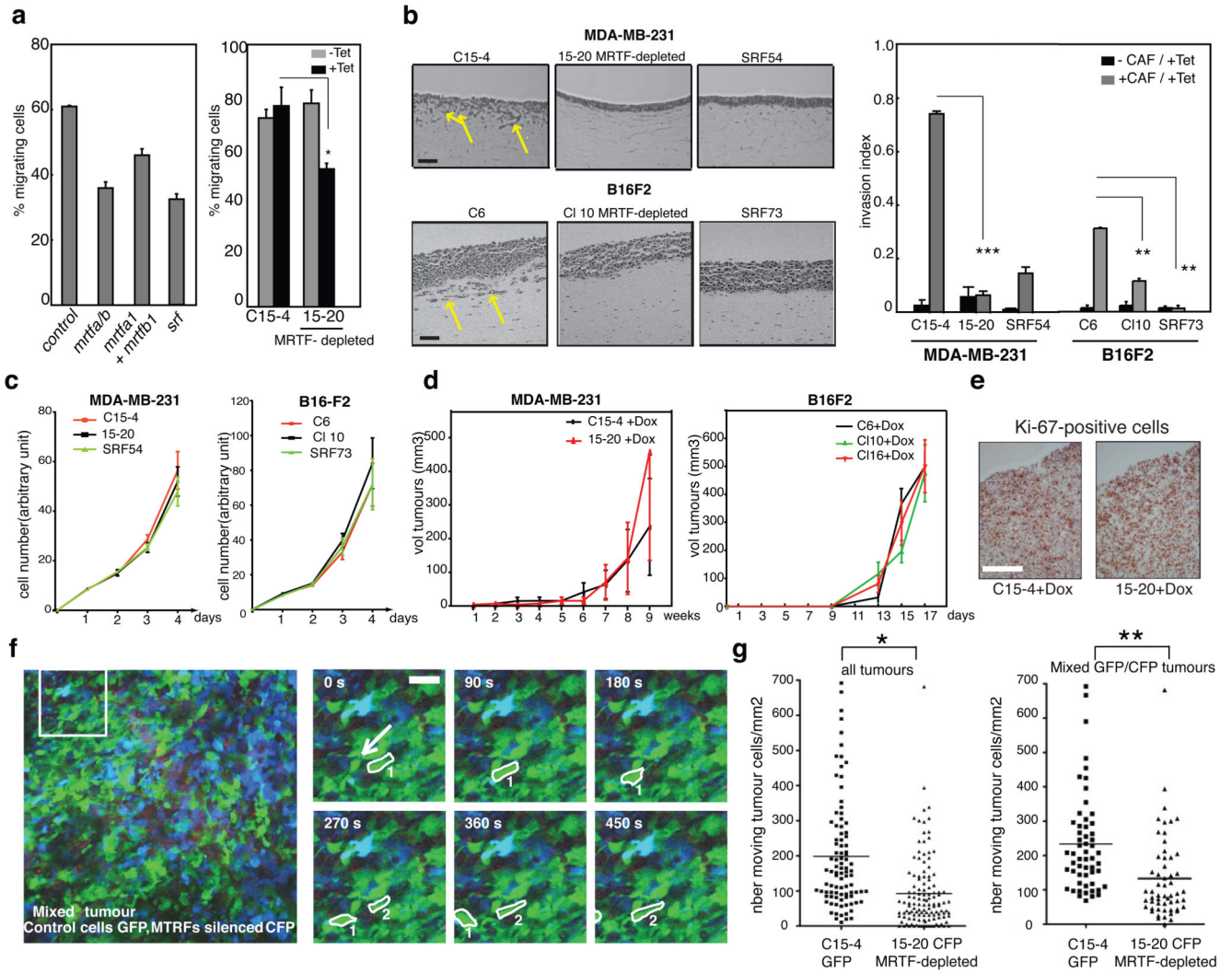
Figure 4. MRTF-SRF signalling is required for invasion and tumour *cell motility in vivo*.
(**A**) MRTF- and SRF-depletion impairs invasion through collagen-coated membrane towards serum-containing medium in the Boyden chamber assay. MRTF and SRF were depleted from MDA-MB-231 cells either by short-term siRNA oligonucleotide transfection in mass culture (left; mean ± half-range, two independent experiments) or in stable cell derivatives expressing tetracycline-inducible MRTF shRNAs (right; mean ± SEM, 3 indepedent experiments; *, P<0.05; Student's t test). (**B**) Fibroblast-led organotypic invasion assay. MDA-MB-231 and B16F2 derivatives were seeded on dense fibrillar collagen I-matrigel matrix containing or lacking embedded carcinoma associated fibroblasts. Invasion was measured after 7 days. Representative H-and-E stained sections; arrows, invading cells; scale bar, 100μm. Data, mean ± SEM, three independent experiments (***, p<0.001; **, p<0.01, Student's t test), except for SRF54 (mean ± half-range, n = 2). (**C**) MRTF or SRF depletion does not affect proliferation of MDA-MB-231 or B16F2 cells cultured with tetracycline (n = 4; 2-way ANOVA: C15-4/15-20, p=0.54; C15-4/SRF54, p=0.91; C6/Cl10, p=0.46; C6/SRF73, p=0.36). (**D**) MRTF does not affect proliferation of MDA-MB-231 or B16F2 cell

xenografts. MDA-MB-231 derivatives (control: C15-4; MRTF-depleted: 15-20) and B16F2 derivatives (control: C6; MRTF-depleted: Cl10, Cl16) were injected subcutaneously into SCID and C57BL/6 mice respectively (12 animals/group); tumour volume was determined weekly (MDA-MB-231) or every other day (B16F2). **(E)** Proliferation status of MDA-MB-231 tumours at 9 wk, revealed by Ki67-staining; scale bar, 250μm. **(F)** Tumour motility *in vivo* monitored by multi-photon confocal imaging. Image shows a mixed tumour: MDA-MB-231 C15-4-GFP parental control cells, green; 15-20-CFP MRTF-depleted cells, cyan; reflectance image, red. Middle panels, 90s time-lapse images of the boxed area, with moving control cells outlined and numbered; arrow, direction of movement. Scale bar, 25μm. **(G)** Quantification of intravital imaging data. Data points, proportion of motile tumour cells in a given confocal section, normalised to the total area of tumour cells in the section (typically 4-6 tumors/animal, 4 areas/tumor, 2-3 sections/area), (*, $p < 0.05$, Mann Whitney test; **$p < 0.01$ Wilcoxon paired test).
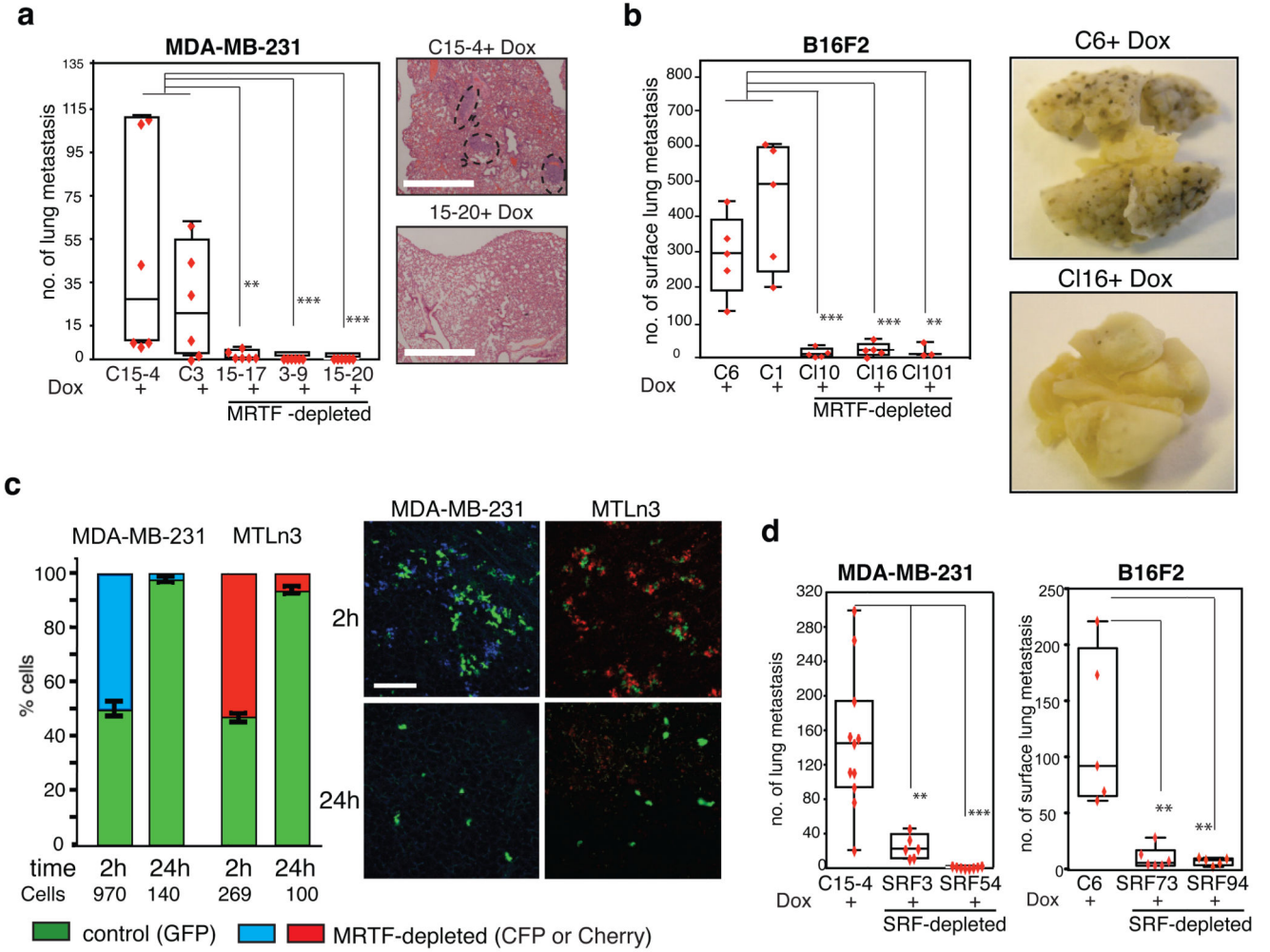
Figure 5. MRTF-SRF signalling is required for an early step in experimental metastasis.
(A) MDA-MB-231 control (C15-4, C3) or MRTF-depleted cells (C15-4 derivatives 15-17, 15-20; C3 derivative C3-9) cells were injected into the tail vein of 5-8 week nude mice (1×10^6 cells each) and maintained with doxycycline. Lungs were isolated after 20 weeks, fixed, and tumour cell nodules in lung sections counted microscopically (6 mice per group; significance by Mann-Wittney test: ***, p<0.001, **, p<0.01). Right, representative H&E-stained lung sections, with tumour nodules outlined by dashes. Scale bar, 250μm. **(B)** Control B16F2 control cells (C6, C1) or MRTF-depleted derivatives of C6 cells (Cl10, Cl16, Cl101), were injected into the tail vein of 5-8 week C57BL/6 mice (0.3×10^6 cells each) and maintained with doxycycline. Lungs were isolated after 14 days and the number of surface tumour nodules quantified as in (A). Right, representative lungs from animals bearing control and MRTF-depleted B16F2 cells. MRTF depletion using a different siRNA combination is shown in Figure S4C. **(C)** Mixtures of GFP-expressing control-transfected and CFP-expressing MRTF-depleted MDA-MB-231 cells (2×10^6 each), or GFP-expressing control-transfected and Cherry-expressing MRTF-depleted MTLn3 cells (0.75×10^6 each) were co-injected into the mouse tail vein, and those present at the lung counted 2h or 24h later. Left, relative proportions of control and MRTF-depleted cells present at 2h or 24h;

total cells detected are indicated below (error bars, SEM; $n = 5$). Right, representative images; scale bar, 50μm. **(D)** Control or SRF-depleted MDA-MB-231 or B16F2 cells were injected into the mouse tail vein of host mice (2×10^6 MDA-MB-231 cells, 6-11 animals; 0.3×10^6 B16F2 cells, 5-6 animals). Lung tumour development was assessed as in panels A and B.

a

	MDA-MB-231			B16F2				
	MRTF depleted / control	control+CD / control	MRTF-depl + CD / control+CD	MRTF-depleted / control	control+CD / control	MRTF-depl + CD / control+CD	MDA-MB-231 MRTF affects	B16F2 MRTF affects
(MYH9)	0.15	1.01	n/a	0.95	1.63	0.59	basal	induced
PDE1C	0.19	0.91	n/a	0.29	0.71	n/a	basal	basal
MYL9	0.25	0.93	n/a	0.36	1.43	0.29	basal	basal, induced
(SDPR)	0.31	0.85	n/a	0.26	0.74	n/a	basal	basal
CYR61	0.47	1.40	0.38	0.82	22.00	0.40	basal, induced	induced
VGLL3	0.48	1.00	n/a	0.25	0.67	n/a	basal	basal
TPM1	0.57	0.99	n/a	0.55	1.06	n/a	basal	basal
HELLS	0.59	0.87	n/a	0.37	0.48	n/a	basal	basal
DENND2A	0.59	1.03	n/a	0.39	0.99	n/a	basal	basal
(PPP1R12A)	0.62	0.98	n/a	0.25	0.61	n/a	basal	basal
(TMEM30A)	0.62	0.88	n/a	0.42	0.50	n/a	basal	basal
PHLDB2	0.64	1.03	n/a	0.25	0.61	n/a	basal	basal
CTGF	0.84	1.34	0.68	0.69	5.82	0.16	induced	basal, induced
FOS	0.98	6.71	0.27	1.74	29.00	0.23	inducted	basal, induced
NR4A1	1.04	2.79	0.41	1.02	4.49	0.47	induced	induced
ZFP36	1.23	1.88	0.64	1.00	3.06	0.54	induced	induced
JUN	1.50	0.80	n/a	1.89	1.76	1.86	basal	basal, induced
YPEL2	1.58	0.91	n/a	1.78	0.63	n/a	basal	basal
GDPD1	1.62	0.83	n/a	2.00	0.93	n/a	basal	basal
BCL6	1.62	1.29	n/a	1.80	1.18	n/a	basal	basal
GLS	1.62	0.98	n/a	1.94	0.75	n/a	basal	basal
HMGA2	2.10	0.98	n/a	2.15	0.75	n/a	basal	basal
FBXO32	2.16	0.86	n/a	2.32	1.01	n/a	basal	basal
KLF4	2.20	1.15	n/a	1.57	2.15	1.69	basal	basal
AMPD3	2.82	0.87	n/a	2.77	0.86	n/a	basal	basal

Figure 6. MRTF-dependent gene expression in MDA-MB-231 and B16F2 cells.
(**A**) MRTF depletion affects both basal-level and cytochalasin D-inducible transcript levels. The transcriptomes of normal and MRTF-depleted B16F2 and MDA-MB-231 cells were analysed by microarray. The table shows genes whose basal and/or CD-induced expression levels change upon MRTF depletion in both lines by more than 1.5-fold (yellow highlight). For CD-induction, the threshold for CD-inducibility was taken as 1.3-fold change over basal (green highlight). Red highlight, SRF target genes validated by previous functional analysis (promoter analysis, ChIP, genetics; for references see13, 42, 43, 50); brackets indicate presumptive SRF targets identified only through conservation of SRF binding sites within 5kb of the transcription start. Microarray data are summarised, and notes on the analysis are given with Supplementary Tables 1A-1D; RT-PCR validation of selected genes is shown in Figure S5A. (**B,C**) MYH9 and MYL9 depletion impairs MDA-MB-231 invasive growth. Cells were depleted of the proteins by transfection of siRNA oligonucleotides, and assayed as in Figure 4A, 4B. (**B**) Boyden chamber assay, performed as in Figure 4A; data are mean ±

half-range, 2 independent experiments. **(C)** organotypic invasion assay, performed as in Figure 4B; data are mean ± half-range, two independent experiments. **(D)** MDA-MB-231-GFP cells were depleted of MYH9 and/or MYL9 by siRNA transfection and injected into the mouse tail vein (0.75×10^6 cells per mouse), and labelled cells in the lung counted 24h later (data are mean ± SEM, n = 4; significance by Mann-Wittney test: *, p<0.05). **(E)** B16F2 cells were depleted of MYH9 and/or MYL9 by siRNA transfection, injected into the mouse tail vein (0.70×10^6 cells per mouse) and lung tumours counted 11 days later (4-5 mice per group; significance by Mann-Wittney test: *, p<0.05).
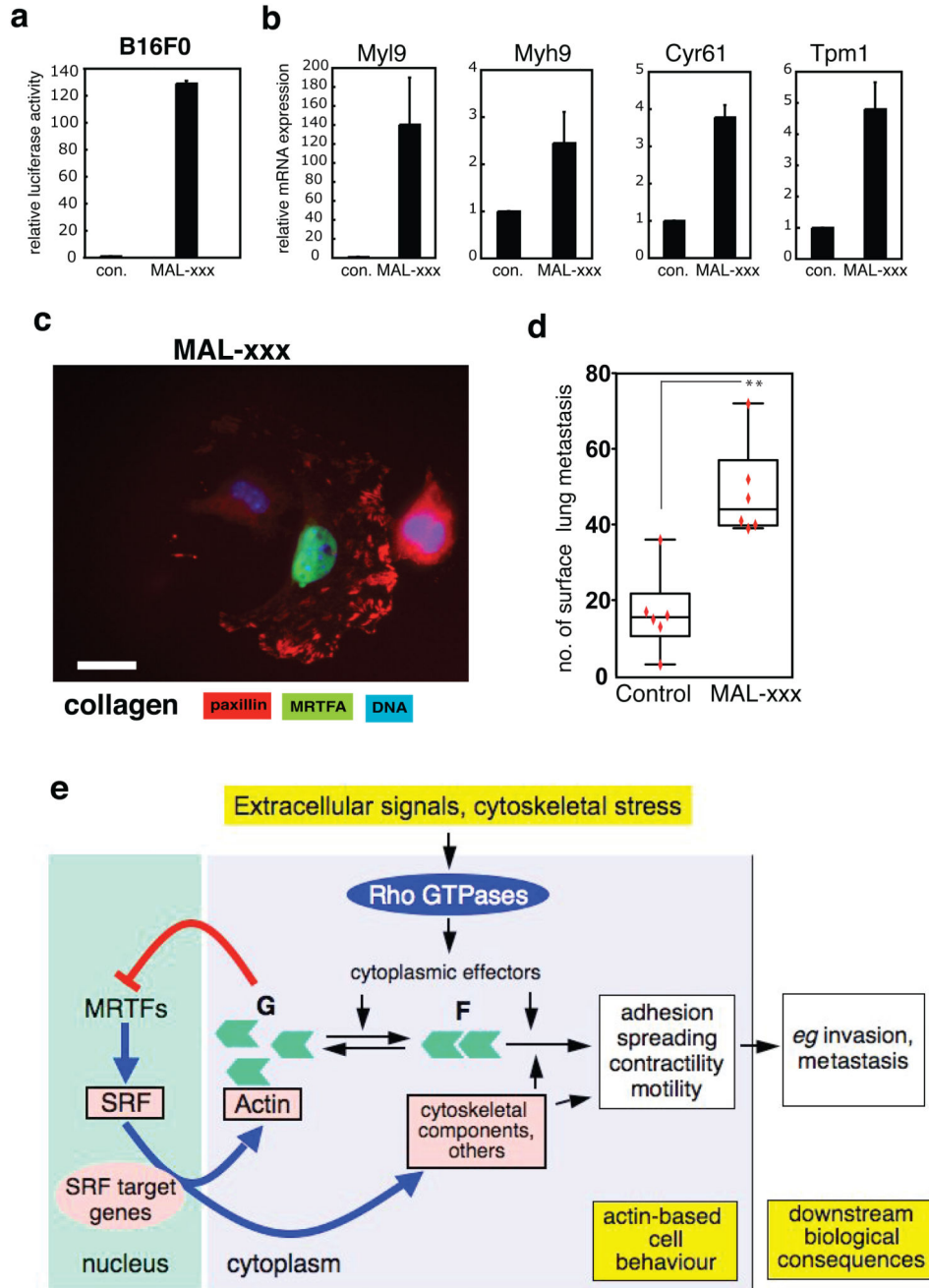
Figure 7. MRTF-dependent gene expression is sufficient to promote experimental metastasis
(A) Activation of the SRF reporter gene in B16F0 cells by co-expression of the activated MRTF-A mutant MAL-xxx[11,12]. A representative experiment is shown; data, mean of duplicate determinations. **(B)** RT-PCR analysis of the endogenous *Myl9*, *Myh9*, *Cyr61*, and *Tpm1* transcripts in B16F0 cells expressing MAL-xxx. Representative of 3 independent experiments; data, mean of duplicate determinations. **(C)** MAL-xxx expression induces a spreading phenotype in B16F0 cells. Cells were plated on collagen and stained for DNA, MRTF-A, and paxillin. Scale bar, 20μm. **(D)** B16F0 cells transfected with MAL-xxx were

injected into the mouse tail vein (0.9×10^6 cells per mouse) and lung tumours counted 12 days later (6 mice per group; significance by Mann-Wittney test: **, p<0.01). **(E)** Schematic representation of the role of Rho GTPase signaling in cytoskeletal rearrangments. Rho GTPases are activated in response to extracellular signals, external (mechanical) cytoskeletal stress and internal homeostatic controls. In the cytoplasm they act directly with effector proteins to control F-actin and G-actin levels through regulation of actin treadmilling, and the assembly and reorganisation of actin-based cell structures1–3 (black arrows). They also signal indirectly to the nucleus to control gene expression through the actin-MRTF-SRF pathway Activity of MRTF proteins is controlled a direct repressive interaction with G-actin (red repressive arrow). Changes in G-actin concentration can be brought about by changes in tonic levels of Rho GTPase activity, or by acute activation in response to signalling, leading to alterations in MRTF activity and consequent changes in SRF-dependent gene expression (blue arrows). This defines a G-actin-MRTF-SRF autoregulatory loop (thick arrows). Our data identify *Myh9* and *Myl9* as among the critical MRTF-SRF targets involved in these processes. Both cytoplasmic and nuclear pathways are required for optimal control of effective cytoskeletal dynamics and their downstream biological consequences.